Improved Photocatalytic Performance of ZnO through AgCu Bimetal Coupling for the Photodegradation of Nitrobenzene

Hauwa Sidi Aliyu[1], Abdul Halim Abdullah[1,2]* and Zulkifly Abbas[3]
[1]Department of Chemistry, Faculty of Science, Universiti Putra Malaysia, 43400 Serdang, Selangor, Malaysia
[2]Materials Synthesis and Characterization Laboratory, Institute of Advanced Technology Universiti Putra Malaysia, 43400 Serdang, Selangor, Malaysia
[3]Department of Physics, Faculty of Science, Universiti Putra Malaysia, 43400 Serdang, Selangor, Malaysia
*Corresponding author (e-mail: halim@upm.edu.my)

A ZnO semiconductor with bimetals (Ag and Cu) coupled in the matrix was successfully prepared using a microwave irradiation technique under a very low synthetic temperature and power of 120ºC and 240 W, respectively. The phase, structural, morphological, and elemental compositions of the synthesized AgCu-ZnO photocatalyst were investigated using transmission electron microscopy, field emission scanning electron microscopy, X-ray diffraction and energy dispersed X-ray and X-ray fluorescence spectroscopy. The band gap energy of the photocatalyst was estimated from the absorption data obtained in UV-Vis spectroscopic analysis. The photodegradation efficiency of the AgCu-ZnO photocatalyst immobilised on a glass plate was evaluated using nitrobenzene (NB) as the model organic pollutant. The immobilized AgCu/ZnO photocatalyst effectively degraded 99% of 20 ppm NB at an optimum catalyst loading of 0.75 g after 2 h of visible light irradiation.

Key words: Photodegradation; AgCu/ZnO photocatalyst; immobilization; nitrobenzene

Received: September 2016; Accepted: May 2017

The development of simpler, faster, low cost and more efficient methods for the complete destruction of persistent organic wastewater pollutants has become very necessary due to the rapid industrialization and globalization in most of the developing countries. Nitrobenzene (NB), is a toxic aromatic organic compound. It is mostly used as the precursor chemical for aniline in the manufacture of textiles, pesticides, rubber materials, pharmaceutical, and cosmetics. It is considered to be a highly toxic organic pollutant and is easily absorbed into the human body through inhalation or skin contact. The symptoms of NB poisoning include general body weakness, headaches, vertigo and sometimes vomiting [1]. Various methods have been employed to remove NB including adsorption, degradation and reverse osmosis and the findings are summarised in Table 1. Except for photocatalysis, other treatment processes have one major drawback in the sense that they only end up transforming the pollutants into a different phase instead of destroying them completely, and these methods may eventually cause a more severe pollution problem (secondary contamination).

Photocatalysis has been considered as one of the most promising techniques for the complete demineralization of persistent organic pollutants in the presence of semiconductor photocatalysts. Among the widely investigated photocatalysts are TiO_2 and ZnO. The irradiation of light onto the surface of the photocatalyst, with an energy higher than the band gap energy, will generate electron-hole pairs. Through a series of reactions, these photogenerated charges produce hydroxyl radicals which then eventually degrade the organic pollutants to harmless by-products such as CO_2 and H_2O. The application of photocatalysis in wastewater treatment, however, has been limited due to the (i) rapid recombination of the electron-hole pairs leading to a significant reduction in photocatalytic performance and (ii) difficulties in separating the photocatalyst from the treated

Table 1. Removal of NB via several wastewater treatment processes.

Process	Findings	Reference
Adsorption	169.4 mg/g of NB was removed when NaOH-modified spent coffee ground was used as an adsorbent.	[4]
	Anthracite, when used as an adsorbent, was capable of removing 0.58 mg/g of NB.	[5]
	Only 2.3 mg/g of NB could be removed by pyrite.	[6]
	Hydroxyapatite-gelatin nanocomposite was able to remove 42.37 mg/g NB	[7]
	Silylated MCM 41 was capable of removing 46.2 mg/g NB	[8]
Osmosis	A polyethersulphate thin film composite membrane was able to reject 76.8% and 55% of 1500 mg/l NB via the forward osmosis and reverse osmosis processes, respectively.	[9]
Degradation	Using a Fenton-like reaction, 1.0 g/l schwertmannite was able to remove 92.5% of 50 mg/l NB within 30 min in the presence of 500 mg/l H_2O_2.	[10]
	Under oxic conditions, 72.3% of 500 mg/l NB could be degraded by 10 g/l Fe/Cu catalyst within 2 h of reaction.	[11]
Photocatalysis	99% of 2.52 x10^{-4} M NB was successfully degraded by 250 mg/l 0.5wt% of a Fe-doped TiO_2 catalyst within 6 h under the medium pressure mercury lamp irradiation.	[12]
	88% of 0.1 mmol NB was removed by a 25 mg $Fe(bpy)_3^{+2}$/ rGO catalyst under 12 h of LED light irradiation.	[13]
	0.75 g of Co/ZnO was able to remove 83% of 20 mg/l NB after 2 h under 18 W fluorescent light irradiation.	[14]

wastewater. Also both TiO_2 and ZnO can only be activated by UV light irradiation.

The photocatalytic activity of a photocatalyst can be improved via metal deposition on the surface of the photocatalyst. The role of metals in photocatalysis is related to the interfacial charge transfer process where they act as electron scavengers, thus reducing the rate of electron-hole pair recombination [2]. Our previous work has shown that the Cu/ZnO photocatalyst was able to photodegrade NB under visible light irradiation [3]. In this work, we aimed to enhance the photocatalytic performance of the ZnO photocatalyst by coupling the photocatalyst with both Ag and Cu. The AgCu/ZnO photocatalyst was prepared *via* microwave irradiation and then immobilised on a glass plate prior to use, for the degradation of NB under visible light irradiation. To the best of our knowledge, the preparation of an immobilised AgCu/ZnO photocatalyst for the degradation of NB under visible light irradiation has not been reported in the literature till date.

METHODOLOGY

Synthesis of the AgCu-ZnO Photocatalyst

11.0 g of zinc acetate dihydrate ($Zn(CH_3OO)_2.2H_2O$), 2.1 g of silver nitrate, and 2.1 g of copper nitrate dihydrate was dissolved in 100 ml of deionised water and was agitated for 15 min. 0.9 g of EDTA, which acts as a complexing agent, was dissolved in 20 ml of deionized water and was added in the solution mixture. The solution mixture was then transferred into a Teflon reaction vessel and irradiated in a microwave oven operating at 120ºC and 240 W for 15 min. The irradiated solution was then removed from the microwave and allowed to cool down naturally. The precipitate that formed was filtered, washed several times with absolute ethanol and deionised water, and then dried in an oven at 60ºC for 6 h.

Immobilisation of the AgCu-ZnO Photocatalyst

The AgCu-ZnO photocatalyst was immobilised onto a glass plate with dimensions of 26 × 76 mm using the spin coating technique. Chitosan solution was prepared by dissolving 0.8 g of chitosan flakes into 120 ml of 1% v/v acetic acid and stirred for 24 h. 5 ml of the chitosan solution was mixed with a certain amount of the photocatalyst and 15 ml of deionised water. The solution was stirred to ensure homogeneity and then coated on the glass plate using a spin coating system (P-6708D).

Characterization of the AgCu-ZnO Photocatalyst

The phase of the prepared photocatalyst was determined using a Shimadzu XRD-6000 diffractometer. The morphology and the elemental composition of the photocatalyst were investigated using a field emission-scanning electron microscope equipped with an energy dispersive X-ray spectrometer (JEOL-JSM-7600F) and a transmission electron microscope (Hitachi H-7100). The elemental composition of the photocatalyst was determined using the X-ray fluorescence spectrometer (Shimadzu EDX-720). The UV-Vis spectrophotometer (PerkinElmer Lambda 35) was used to determine the band gap energy of the photocatalyst.

Photodegradation Procedure

A glass plate coated with a certain amount of the AgCu-ZnO photocatalyst was immersed in 20 ppm, 1.0 L NB solution. The solution was stirred in the dark for 45 min to ensure that the adsorption equilibrium was achieved. The light source (23 W Philip bulb) was then switched on and at specific time intervals, a sample aliquot was withdrawn from the bulk solution and filtered through a 0.45 μm polytetrafluoroethylene membrane filter. The samples were analysed using the UV-Visible spectrophotometer (Shimadzu, UV-1650 PC) at λ_{max} = 267.5 nm to determine the concentration of NB in the sample. The photodegradation percentage of the NB was calculated as follows;

$$\text{Photodegradation } \% = \frac{C_0 - C_t}{C_0} \times 100 \qquad (1)$$

where, C_0 = Initial concentration of NB; C_t = concentration of NB at time t of photo irradiation. The progress of the photodegradation was also monitored using the total organic carbon analyzer (TOC, Shimadzu). All the photodegradation experiments were carried out in a triplet.

RESULTS AND DISCUSSION

Structural Morphology and Phase Study

The FESEM images, illustrated in Figure 1 (a), revealed that the AgCu/ZnO photocatalyst had irregularly shaped and rod-like particles with both the Ag and Cu metals attached on the surface of the ZnO nanorods. Figure 1b shows the XRD pattern of the AgCu/ZnO photocatalyst. The XRD peaks were characteristic of hexagonal ZnO, which was in accordance with the International Centre for Diffraction Data (Reference Code: 98-004-0985), face-centred-cubic Ag metal (Ref Code: 98-008-4046) and face-centred-anorthic Cu metal (Ref Code: 98-011-5831) indicating the purity and crystallinity of the sample.

Elemental Composition

The EDX spectrum obtained from a selected area of the FESEM image is shown in Figure 2a. The AgCu/ZnO photocatalyst consisted of only Zn, Ag, Cu and O thus further confirming the purity of the sample. The peaks attributed to $L_{\alpha\alpha1}$, $K_{\alpha1}$, and $K_{\beta1}$ of Zn were observed at 1.0, 8.6 and 9.6 keV, respectively. This indicated that the coupling of the metals into the matrix of the ZnO semiconductor did not affect the structural and morphological properties of the actual ZnO material. Using XRF analysis (*via* an easy-air–oxide method), the photocatalyst was found to contain 62.4 wt% Zn,

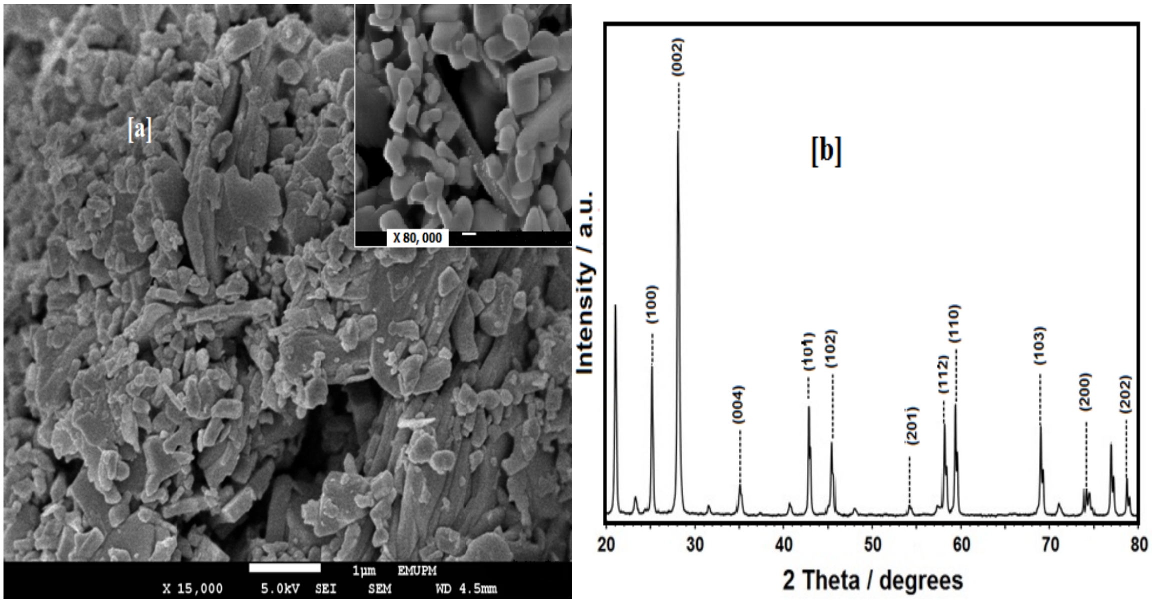

Figure 1 (a). Low and highly magnified FESEM image and (b) XRD pattern of the AgCu/ZnO photocatalyst.

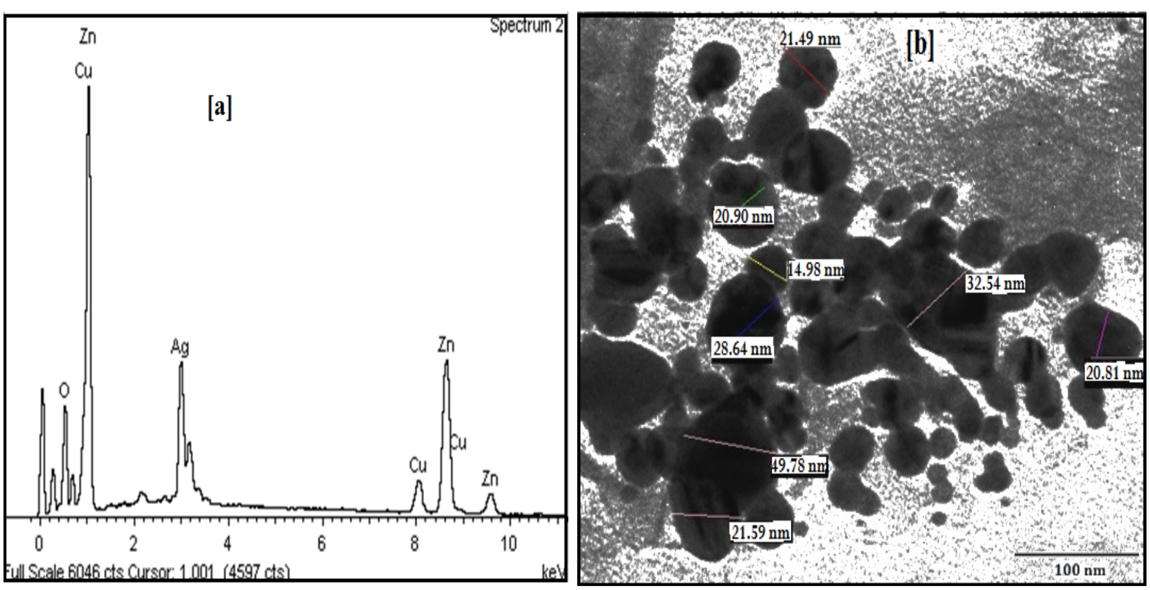

Figure 2 (a). EDX spectrum and (b) TEM image of the AgCu/ZnO photocatalyst.

24.8 wt% Cu and 12.8 wt % Ag. TEM images of the AgCu/ZnO photocatalyst shown in Figure 2b revealed that the size of the particles was less than 100.0 nm.

The UV-Vis spectrum of the photocatalyst showed a peak with a λ_{max} of 378.0 nm. Using the Kubelka-Munk transformation function, the absorbance data was used to determine the band gap of the photocatalyst. The inset diagram in Figure 3 shows a plot of $(Ah\nu)^2$ as a function of photon energy, hν. The band gap energy, estimated from the intercept of the tangent at the x-axis, was found to be 2.85 eV which indicated that the catalyst could be activated by visible light irradiation.

Photodegradation of NB

The determination of the maximum photocatalyst loading is of utmost importance when conducting any type of heterogeneous photocatalytic reaction to avoid excessive usage. The effect of photocatalyst loading in the photodegradation efficiency of NB is shown in Figure 4a. The results revealed an increase in photodegradation efficiency up to 99% with an increase in the mass loading from 0.25 g to 0.75 g before declining with the further increase in mass load to 1.00 g. The decrease could be attributed to the agglomeration of the photocatalyst. Figure 4b revealed a reduction in the photodegradation percentage of NB as the NB concentration increased. This could be due to the unavailability of the active sites of the photocatalyst as they were covered with nitrobenzene at higher concentrations. Since the photocatalysis relies on the absorption of light by the photocatalyst, both the agglomeration and strong adsorption of NB on the surface of the photocatalyst would reduce the light absorption capacity of the photocatalyst. As a result, a lower number of electron-hole pairs were generated leading to a reduction in the hydroxyl radicals formed and consequently, a decrease in the photodegradation efficiency [15]. Another possibility was that the amount of radical species formed at the surface of the photocatalyst tended to be constant at constant photocatalyst mass, illumination time and light intensity. Therefore, the relative ratio of the radical species available to degrade NB decreased with increasing NB concentration which led to a reduction in the photodegradation percentage [16]. Pannee *et al*., and Pardeshi and Patil [17,18] reported similar findings. The increase in NB concentration could also result in the generation of reaction intermediates which could adsorb on the photocatalyst surface, leading to the deactivation of the photocatalyst and a reduction of the overall photodegradation rate.

Kinetics of Photocatalytic Mechanism of the Nitrobenzene

Heterogeneous photocatalytic reactions can be analysed using a modified Langmuir-Hinshelwood model (L-H model) [19].

$$r = \frac{-dC}{dt} = \frac{k_r KC}{1+KC_0} = k_{obs}C \tag{2}$$

Equation (2) can be rewritten as

$$\frac{1}{k_{obs}} = \frac{1}{k_r K} + \frac{C_0}{k_r} \tag{3}$$

By integrating Equation 2, a typical pseudo-first-order equation can be obtained as follows:

$$\ln\frac{C_0}{C} = k_{obs}C \tag{4}$$

where, k_{obs} is the apparent pseudo first order rate constant, C = NB concentration in the solution at a given irradiation time t, C_0 = initial NB concentration. Figure 5a shows a plot of $\ln\frac{C_0}{C}$ vs time for the degradation of NB at different initial NB concentrations. The k_{obs} values, obtained directly from the regression analysis of the curve, are listed in Table 2.

The data obtained indicated that the degradation of NB at higher concentrations fit the pseudo first order reaction better than that at lower concentrations. A plot of $\frac{1}{k_{obs}}$ *versus* initial NB concentration, C_0, (Figure 5b), was a straight line, confirming a good correlation between the Langmuir-Hinshelwood model and the rate of NB degradation.

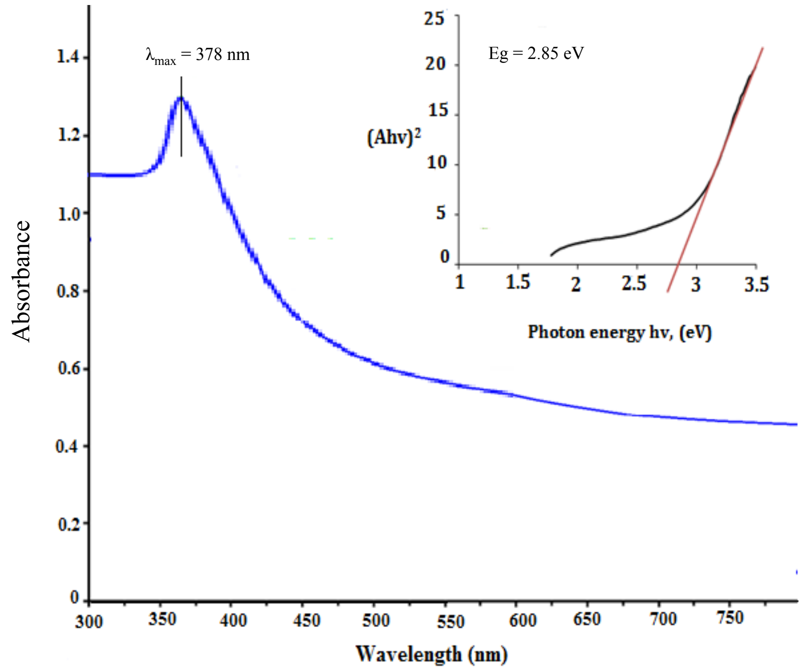

Figure 3. Absorption spectrum and Tauc's plot for band gap energy determination of the AgCu/ZnO photocatalyst.

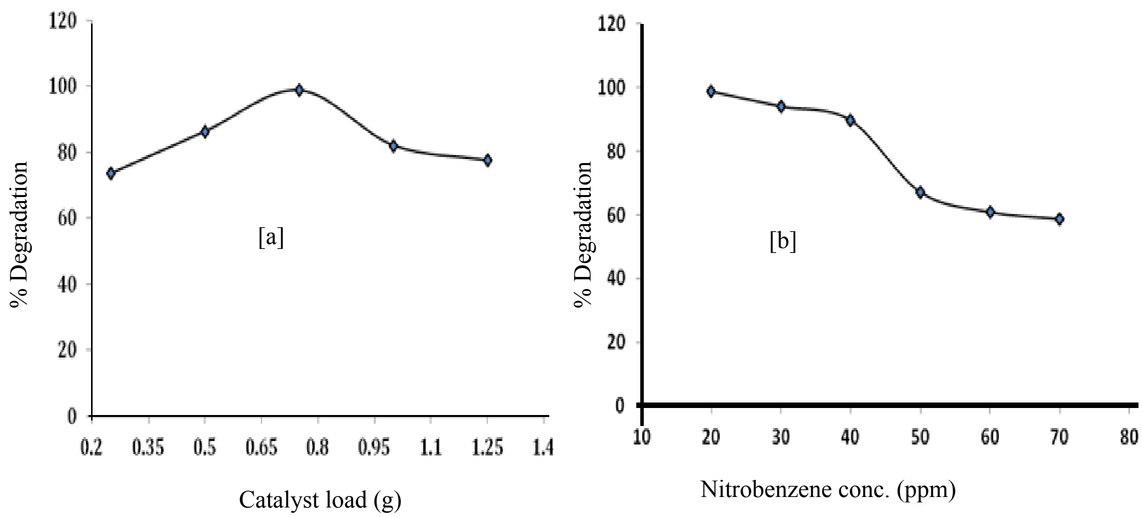

Figure 4. Photocatalytic degradation of NB by the AgCu/ZnO photocatalyst at different (a) catalyst mass loading and (b) initial NB concentration. Experimental conditions: mass of AgCu/ZnO = 0.75 g, initial concentration of NB = 20 ppm, pH=7.43.

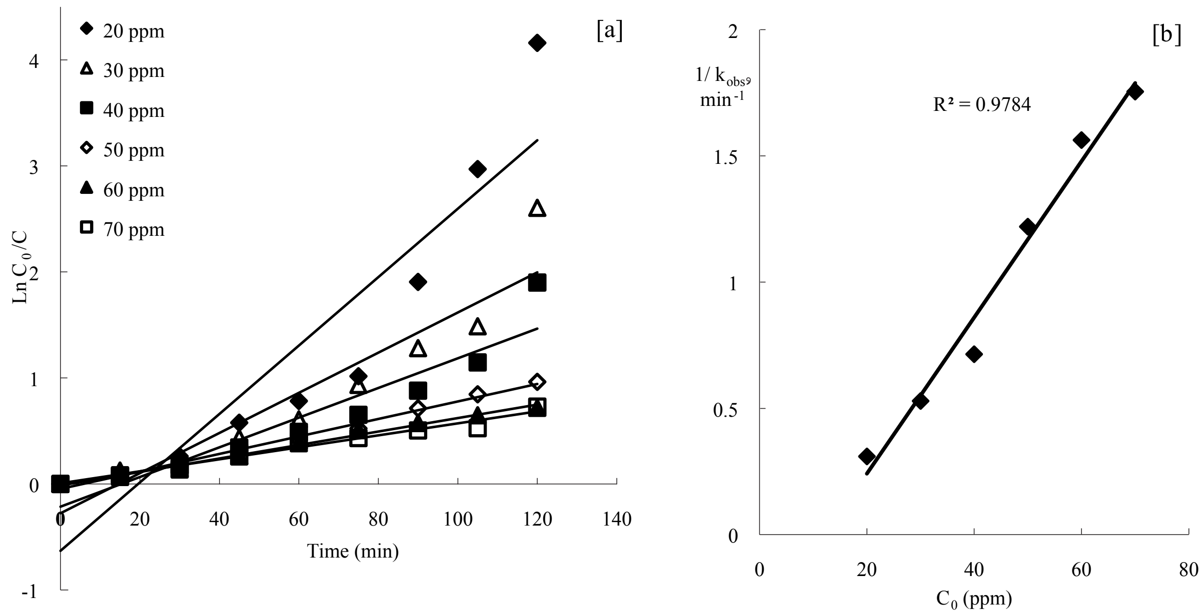

Figure 5 (a). Photodegradation of NB by the AgCu/ZnO photocatalyst and (b) variation of the reciprocal rate constant at different NB concentrations. Conditions: Mass of catalyst = 0.75 g, concentration of NB = 20–70 ppm, pH = 7.43.

Table 2. Apparent rate constants for the degradation of NB at different initial concentrations

C_0 (ppm)	$k_{obs} \times 100$ (min^{-1})	R^2
20	3.23	0.8537
30	1.89	0.8800
40	1.40	0.8854
50	0.82	0.9914
60	0.64	0.9908
70	0.57	0.9754

TOC Removal and Reusability

The progress of NB degradation by the AgCu-ZnO photocatalyst was also monitored via the total organic carbon (TOC) concentration. Figure 6a shows that 92% of the organic carbon was degraded by 0.75 g of the catalyst. This value was slightly lesser than that observed from UV-Vis analysis (99%) indicating the presence of intermediates that required a longer time to be degraded by the photocatalyst.

The reusability of the photocatalyst was investigated by keeping all the experimental parameters constant. At the end of the first cycle, the catalyst was rinsed several times with deionized water and dried at 60ºC in an oven for 6 h before being used in the next cycle. As shown in Figure 6b, a slight reduction in degradation percentage was observed after 2 cycles. The decrease could be attributed to the adsorption of the intermediates on the surface of the photocatalyst as confirmed through the TOC analysis. However, the sample catalyst was able to retain its good photodegradation performance (85%) even after four cycles, supporting the reusability of the photocatalyst in the degradation of NB in aqueous solution.

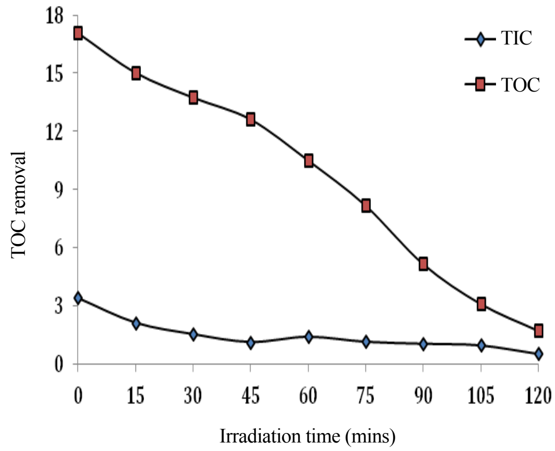

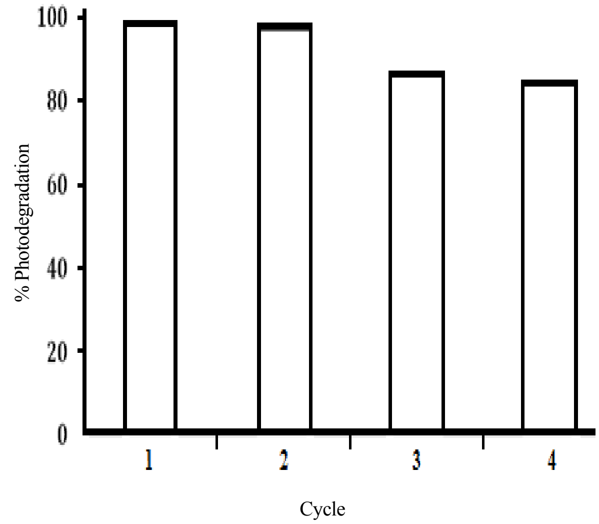

Figure 6 (a). Total organic carbon removed and (b) the reusability of the AgCu-ZnO photocatalyst in the photodegradation of NB. Experimental Conditions: Mass of catalyst = 0.75 g, NB concentration = 20 ppm, pH = 7.43.

CONCLUSIONS

The microwave irradiation technique was an efficient method for the preparation of a ZnO photocatalyst with bimetals (Ag and Cu) coupled in the matrix. The addition of both Ag and Cu into the ZnO matrix did not affect the structural and morphological properties of ZnO but reduced the band gap energy and enhanced the light absorption capacity of ZnO in the visible region. The immobilized AgCu/ZnO photocatalyst exhibited the highest degradation efficiency of 99% when 0.75 g of the catalyst was used to degrade 20 ppm NB within 2 h under visible light irradiation. The immobilized photocatalyst was also found to be stable and showed a slight decrease in photocatalytic performance after being used for three cycles.

ACKNOWLEDGEMENTS

The authors acknowledge the financial support from the Ministry of Higher Education, Malaysia (FRGS-5524150) for this work.

REFERENCES

1. Whang, T-J., Hsieh, M-T. and Chen H-H. (2012) Visible-light photocatalytic degradation of methylene blue with laser-induced Ag/ZnO nanoparticles, *Applied Surface Science*, **258**, 2796–2801

2. Curri, M., Comparelli, R., Cozzoli, P., Mascolo, G. and Agostiano, A. (2003) Colloidal oxide nanoparticles for the photocatalytic degradation of organic dyes, *Journal of Material Science and Engineering*, **C 23**, 285–289

3. Sidi, H.A., Abdullah, A.H. and Abbas, Z. (2015) Enhanced photocatalytic efficiency of microwave synthesized Cu/ZnO photocatalyst, *International Journal of Multidisciplinary Research and Development*, **2(3)**, 612–615

4. Dai, Y., Zheng, D. and Zhang, K. (2016) Nitrobenzene adsorption capacity of NaOH modified spent coffee ground from aqueous solution, *Journal of the Taiwan Institute of Chemical Engineers*, **68**, 232–238.

5. Parsham, H. and Saeed, S. (2013) Simultaneous removal of nitrobenzene, 1,3 dinitrobenzene and

2,4 dichloronitrobenzene from water sample using anthracite as a potential adsorbent. *Journal of Environmental Chemical Engineering*, **1**, 1117–1123.

6. Zhang, Y, Zhang, K., Dai, C. and Zhou, X. (2014) Performance and mechanism of pyrite for nitrobenzene removal in aqueous solution, *Chemical Engineering Science*, **111**, 135–141.

7. Wei, W., Sun, R., Jin, Z., Cui, J. and Wei, Z. (2014) Hydroxyapatite-gelatin nanocomposite as novel adsorbent for nitrobenzene removal from aqueous solution, *Applied Surface Science*, **292**, 1020–1029.

8. Dong, Q. and Xu, Y, (2016) Enhanced nitrobenzene adsorption on aqueous solution by surface silylated MCM 41, *Microporous and Mesoporous Materials*, **232**, 143–150.

9. Cui, Y., Liu, X-Y., Chung, T.S., Weber, M., Staudt, C. and Maletzko, C. (2016) Removal of micropollutant (phenol, aniline and nitrobenzene) via forward osmosis (FO) process: evaluation of FO as alternative method to reverse osmosis (RO), *Water Research*, **71**, 104–114.

10. Duan H, Liu, Y., Yin, X., Bai, J. and Qi J. (2016) Degradation of nitrobenzene by fenton-like reaction in a H_2O_2/schwertmannite system, *Chemical Engineering Journal*, **283**, 873–879.

11. Sun, L., Song, H., Li, Q. and Li, A. (2016) Fe/Cu bimetallic catalysts for reductive degradation of nitrobenzene under oxic condition, *Chemical Engineering Journal*, **283**, 366–374.

12. Nitoi, I., Oancea, P., Raileanu, M., Crisan, M., Constantin, L. and Cristea, I. (2015) UV-Vis photocatalytic degradation of nitrobenzene from waster using heavy metal doped titania, *Journal of Industrial and Engineering Chemistry*, **21**, 677–682.

13. Kumar, A., Kumar, P., Paul, S. and Jain, S.L. (2016) Visible light assisted reduction of nitrobenzene using Fe(Bpy)3+2/rGO nanocomposite as photocatalyst, *Applied Surface Science*, **386**, 103–114.

14. Liman, M.G., Abdullah, A.H., Hussein, M.Z. and Zainal, Z. (2014) Photodegradation of nitrobenzene using cobalt modified zinc oxide particle, *Asian Journal of Chemistry*, **26**, S287–S290.

15. Konstantinuou, I. and Albanis, T. A. (2004) TiO_2-assisted photocatalytic degradation of azo dyes in aqueous solution: kinetic and mechanistic investigations, *Journal of Applied Catalysis on the Environmental*, **B49**, 1–14

16. Gaya, U. and Abdullah, A. (2008) Heterogeneous photocatalytic degradation of organic contaminants over titanium dioxide: A review of fundamentals, progress and problems, *Journal of Photochemistry and Photobiology C: Photochemistry Reviews*, **9**, 1–12.

17. Pannee, A., Chradda, B. and Wichien, S. (2012) Photocatalytic activity under solar irradiation of silver and copper doped zinc oxide: photodeposition versus liquid impregnation methods, *Journal of Applied Sciences*, **12**, 1809–1816.

18. Pardeshi, S. K. and Patil, A. (2008) A simple route for photocatalytic degradation of phenol in aqueous zinc oxide suspension using solar energy, *Journal of Solar Energy*, **82**, 700–705.

19. Khezrianjoo, S. and Revanasiddappa, H.D. (2012) Langmuir-Hinshelwood kinetic expression for the photocatalytic degradation of metanil yellow aqueous solution by ZnO catalyst. *Chemical Sciences Journal*, **3**, 1–8.